Atmos. Chem. Phys. Discuss., 9, 13407–13437, 2009
www.atmos-chem-phys-discuss.net/9/13407/2009/

Atmospheric Chemistry and Physics Discussions

This discussion paper is/has been under review for the journal *Atmospheric Chemistry and Physics (ACP)*. Please refer to the corresponding final paper in *ACP* if available.

Annual particle flux observations over a heterogeneous urban area

L. Järvi[1], Ü. Rannik[1], I. Mammarella[1], A. Sogachev[2], P. P. Aalto[1], P. Keronen[1], E. Siivola[1], M. Kulmala[1], and T. Vesala[1,3]

[1]Department of Physics, P.O. Box 64, 00014 University of Helsinki, Finland
[2]Risø National Laboratory for Sustainable Energy, Technical University of Denmark, P.O. Box 49, 4000 Roskilde, Denmark
[3]Department of Forest Ecology, P.O. Box 27, 00014 University of Helsinki, Finland

Received: 24 April 2009 – Accepted: 8 June 2009 – Published: 17 June 2009

Correspondence to: L. Järvi (leena.jarvi@helsinki.fi)

Published by Copernicus Publications on behalf of the European Geosciences Union.

Abstract

Long-term eddy covariance (EC) particle number flux measurements for the size range 6 nm to 5 µm were performed at the SMEAR III station over urban area in Helsinki, Finland. Heterogeneous urban environment allowed us to study the effect of different land-use classes in different wind directions on the measured fluxes. The particle fluxes were observed to be the highest from the road direction during weekdays with day-time median flux 0.8×10^{9} m^{-2} s^{-1}. Particle fluxes showed a clear dependence on traffic rates and mixing conditions of the boundary layer. In the direction of road, the larger particle fluxes were dominated by smaller sizes. Footprint analysis was performed by using numerical modeling and emission rate of particles from road was estimated to be 0.8×10^{12} s^{-1} m^{-1} during day-time. With typical traffic rate of 2500 vehicles per hour this corresponds to average emission rate of 1.2×10^{15} vehicles^{-1} km^{-1}. The particle fluxes from vegetated area were the lowest with daytime median fluxes below 0.2×10^{9} m^{-2} s^{-1}. During weekends and nights the particle fluxes were low from all land use sectors being in the order of $0.02–0.1\times10^{9}$ m^{-2} s^{-1}. On annual scale, the highest fluxes were measured in winter when emissions from stationary combustion sources are higher.

1 Introduction

Atmospheric aerosols are known to have adverse health effects especially in urban areas (Curtis et al., 2006; Keeler et al., 2005), where many of the pollution sources are located and where large amount of people are exposed to these pollutants. Aerosol particles affect also climate by directly either cooling or warming the atmosphere depending on the particle composition, or indirectly acting as cloud condensation nuclei and further affecting the radiation balance of Earth (Intergovernmental Panel on Climate Change, 2007). In urbanized areas, road traffic has been identified to be the main source especially for ultrafine particles, which can be either primary or secondary ones

due to condensation from exhaust gases (e.g. Thomas and Morawska, 2002; Young and Keeler, 2007; Järvi et al., 2009). Besides traffic, also other combustion sources are relevant for particle emissions (e.g. Pakkanen et al., 2001; Young and Keeler, 2007), and especially in cold regions wood burning can cause high emissions in winter time (e.g. Glasius et al., 2006). Despite the fact that many of the sources of atmospheric particles have been identified, there is still lot of uncertainty in the emission strength of different sources and their contribution on particle concentrations, especially on scale related to micrometeorological flux measurements.

In natural ecosystems, lot of work related to particles exchange between the ecosystem and atmosphere has been made, while in cities studies are limited as was reviewed by Pryor et al. (2008). Few studies have concentrated on modelling the particle emissions in urban areas via different methods (e.g. Palmgren et al., 1999; Kumar et al., 2008), while the direct particle flux measurements have been made in a few cities with shorter campaigns (Nemitz et al., 2000; Dorsey et al., 2002; Longley et al., 2004a; Longley et al., 2004b; Donateo et al., 2006; Mårtensson et al., 2006; Martin et al., 2008; Nemitz et al., 2008; Schmidt and Klemm, 2008). Particle exchange measurements provide important information on the previously mentioned emission strengths and distributions of sources, and in addition yield input parameters on air quality and climate models. Recently, Schmidt and Klemm (2008) were the first one to report size-resolved particle fluxes in the city of Münster in Germany, while Nemitz et al. (2008) reported the first results on fluxes of chemical species of particulate matter from Boulder, Colorado.

In Helsinki, Finland, the continuous measurements of particle number fluxes with the eddy covariance (EC) technique were started at the urban measurement station SMEAR III in July 2007. EC provides the most direct way to measure the atmospheric exchange, and the measurement system was able to detect particles starting from 6 nm up to 5 µm in aerodynamic diameter. Main particle sources in Helsinki have identified to be energy production, road traffic and wood burning accounting 32, 28 and 29 mass percentage of the total particle emissions, which were estimated to be 1042 tons year^{-1} in 2007 (Niemi et al., 2008). The complex measurement site provides a possibility

to study the effect of land use on the particle exchange, while the northern location enables to analyze the fluxes in varying meteorological conditions with distinguishable seasons. Thus, the main purpose of this study is to analyze the effect of land use and the temporal behaviour of the flux up to seasonal time scale. The influence of traffic rate on particle number fluxes, the relationship between particles sizes and fluxes as well as the correlation of particle and carbon dioxide fluxes are also studied.

The emission rate, defined by the negative ratio of flux to concentration, is a frequently used variable employed in the analysis and characterisation of particle exchange over urban areas (e.g. Dorsey et al., 2002). It is well known that flux and concentration have very different source weight functions called footprint functions (e.g. Schmid, 2002), the concentration footprint function giving more weight to distant sources. In addition the aerosol particle concentration contains significant background component, which is determined by sources other than those inducing the flux. Also, concentrations are more affected by atmospheric mixing and observation height; particle flux is more invariant with respect to chosen observation height and turbulence conditions. To avoid such complications and to have more general description of local particle sources and sinks we chose to analyse the particle fluxes instead of emission velocities.

2 Measurements and methods

2.1 Site description

The measurements of aerosol particle number fluxes with the eddy covariance (EC) technique were made at the urban measurement station SMEAR III (*Station for Measuring Ecosystem – Atmosphere Relationships*) in Helsinki, Finland, between July 2007 and July 2008. The measurements were made on the top boom of a 31 m high triangular lattice tower situated on a hill (60°12′ N, 24°57′ E, 26 m from sea level) around 5 km north-east from the Helsinki centre. The measurement surrounding is heteroge-

neous consisting of buildings, paved areas and vegetation (Fig. 1), and it was divided into three land use sectors according to a typical land use on the area. The urban sector, which is mainly covered with buildings (mean height 20 m), roads and parking lots, is located in direction 320–40°. The road sector is in direction 40–180° and one of the main roads leading to the Helsinki city centre with traffic rate of 45 000 vehicles day^{-1} on workdays (Lilleberg and Hellman, 2008) passes the sector at a distance of 150 m from the tower. The vegetation sector in direction 180–320° is mainly covered with vegetation at both University Botanical garden and allotment garden. More detailed description about the measurements site can be found from Vesala et al. (2008) and Järvi et al. (2009).

2.2 Measurements

The EC measurement setup consisted of a Metek ultrasonic anemometer (USA-1, Metek GmbH, Germany) to measure all three wind velocity components and sonic temperature, and a water-based condensation particle counter (WCPC, TSI-3781, TSI Incorporated, USA) to measure aerosol particle number concentration. The 50% cut-off size of WCPC is 6 nm. In addition, particle losses occur in sampling line mainly due to Brownian diffusion and impaction mechanisms prevailing at small and large particle sizes, respectively. However, measurements at small particle sizes were limited by WCPC ability to detect small particles and not by the sampling line as can be seen from the particle size transfer function of the EC system (Fig. 2).

CO_2 mixing ratios to be used in CO_2 flux calculations were measured with a closed-path infrared gas analyzer (LI-7000, LI-COR Biosciences, USA). Both the aerosol particle and CO_2 analyzers used the same air inlet situated 13 cm below the anemometer. The inlet was covered with a 6 mm diameter filter (mesh 0.1 mm) and rain cover. The main tube connected to CO_2 analyzer was a 40 m long steel tube with inner diameter of 8 mm. The side flow to the WCPC was drawn with a 0.1 m long tube from the main tube at a distance of 3.6 m from the inlet. The air flow in the main tube was 16 l min^{-1} and it was heated to avoid water condensation on the walls. Time lags and fluxes

of aerosol particles and CO_2 were determined with a maximum covariance technique (e.g. McMillen, 1988). EC measurements were recorded with 10 Hz.

The aerosol particle size range from 3 to 950 nm was measured with a twin Differential Mobility Particle Sizer (DMPS, Aalto et al., 2001) in a container situated next to the measurement tower. Our setup consisted of a Hauke-type DMA (10.9 cm in length) and a TSI Model 3025 Condensation Particle Counter (CPC) to measure size range 3–50 nm, and a Hauke-type DMA (28 cm in length) and a TSI Model 3010 CPC to measure size range 10–950 nm. For the first system, the sample and sheath flows were 4 and 20 l min^{-1}, respectively, and for the second system, 1 and 5 l min^{-1}, respectively. Each sheath flow was arranged as a closed loop with an air filter and aerosol dryer. The sampling line was a 2 m long stainless steel tube with inner diameter of 4 mm and flow rate 4 l min^{-1}, and it was drawn outside the measurement container from a height of 4 m from the ground. The measurement resolution for the combined system was 10 min. Data was recorded and will be presented in Eastern European Time (EET), so that no summer time correction was included.

The measurement period was divided into three seasons: summer, fall/winter and spring. Winter was not separated from fall since no thermal winter (daily average temperatures below 0°C over 5 d) was observed during the measurement period. The summer period covered July–August 2007 and June–July 2008, the fall/winter period September 2007–March 2008 and the spring period April–May 2008.

2.3 Traffic monitoring

Traffic rates in Helsinki area are monitored by the Helsinki City Planning Department. The nearest on-line traffic calculation point is by the Itäväylä road about 2.5 km South-East from the measurement station. The traffic patterns in Itäväylä and road next to the measurement station are similar except the traffic rates are 25% higher in Itäväylä (Lilleberg and Hellman, 2008). This difference was taken into account when analysing data. Traffic data was logged every hour except during rush hours when it was logged four times in hour. Due to the limited amount of traffic data, data analysis including

traffic data covered only period July 2007–May 2008

2.4 Data processing

With the EC technique a 30-min turbulent flux F_s is calculated as a covariance between vertical wind speed w and scalar s according to equation

$$F_s = \overline{w's'}. \quad (1)$$

In our case, s was either aerosol particle concentration or mixing ratio of CO_2. Before the flux calculation, data was linearly de-trended and a 2-dimensional coordinate rotation was applied. To improve particle flux data, quality observation periods with clear spikes in particle concentration records as detected by visual inspection were excluded. In addition, analysed data were selected according to friction velocity greater than 0.1 m s^{-1} to avoid low turbulence conditions. The co-spectral corrections were applied to particle and CO_2 fluxes, and the attenuation factors were calculated numerically integrating

$$\frac{F_s}{F} = \frac{\int_0^\infty TF_{\mathrm{High}}(f)TF_{\mathrm{Low}}(f)C_{ws}(f)df}{\int_0^\infty C_{ws}(f)df}, \quad (2)$$

where F_s and F are the measured and un-attenuated fluxes, respectively, f is the natural frequency, $TF_{\mathrm{High}}(f)$ and $TF_{\mathrm{Low}}(f)$ are the transfer functions at the high- and low frequency ends, respectively, and $C_{ws}(f)$ is the co-spectral density describing the frequency behaviour of the turbulent flux (Moore, 1986; Horst, 1997). The co-spectral models of Kaimal et al. (1972) for sensible heat were used as $C_{ws}(f)$, and the normalized frequency n_m at which the frequency weighted co-spectrum $fC_{ws}(f)$ attains its maximum value was determined experimentally as a function of atmospheric stability $\zeta = \frac{z-d}{L}$, where L is the Obukhov length, z is the measurement height and d is the displacement height defined separately for each land use sector (13, 8 and 6 m for urban,

road and vegetation, respectively). In unstable cases, n_m was found to be constant with a value of 0.1±0.04 (SD), and in stable cases a fitting in a least-square sense was made yielding (Fig. 3)

$$n_m = 0.1\left(1+1.6\zeta^{0.17}\right). \quad (3)$$

For the low frequency loss, $TF_{\mathrm{Low}}(f)$ associated with linear de-trending was used (Rannik and Vesala, 1999), while for $TF_{\mathrm{High}}(f)$ the following co-spectral transfer function was employed

$$TF_{\mathrm{High}}(f) = \frac{1}{1+(2\pi\tau_c f)^2}, \quad (4)$$

where the first order response time τ_c was determined experimentally from the ratio of normalized co-spectral density of respective scalar and sensible heat (Rannik et al., 2004). The experimental transfer function for aerosol particle number fluxes was calculated from 270 half hourly data runs measured in March–June 2008 and a value of τ_c=0.5 s was obtained.

2.5 Footprint analysis

Over complex topography and heterogeneous terrain the only possible way to estimate the influence of surface sources to measured flux is via numerical calculations. The footprint simulations were performed by using the numerical atmospheric boundary-layer model SCADIS (Sogachev and Lloyd, 2004; Sogachev et al., 2004; Sogachev and Panferov, 2006). The model is based on a one-and-a-half-order turbulence closure applying E–ω scheme, where E is the turbulent kinetic energy and ω is the specific dissipation of E (Sogachev et al., 2002; Sogachev, 2009). In simulations, the land use was classified into nine different types including roads, parking areas, soil, and trees with two different height classes and buildings with four different height classes. Buildings were considered as impenetrable. Footprint calculations were done for the

road sector with inflow geostrophical wind from direction 117° and speed 10 m s^{-1} and by assuming a neutral stratification. The cell size of simulations was 20×20 m^2.

3 Results

In urban conditions, the particle fluxes are expected to follow several drivers. The fluxes depend on wind direction due to different surface types; also seasonal and diurnal variation is likely to exist in measured fluxes. In the following these dependencies are studied in more detail.

3.1 Particle flux dependence on wind direction

Figure 4 indicates that the highest particle fluxes occurred when wind was between East and South, the direction corresponding to the road sector. In winter, the largest particle fluxes were measured from South, in spring from South-East and in summer the fluxes were more evenly distributed between Eastern and Southern directions. In winter and spring, relatively high fluxes were observed also from North, where a parking lot close to measurement point is located. Car emissions from parking lot could explain also the seasonality of this local directional maximum, since activity at parking lot is lower in summer due to summer vacations. Residential area with one family houses is also located in North, where wood burning for heating could contribute to such dependence during colder months.

Differences between seasons could be observed also in other directions. In winter, the fluxes from South and from direction 60–90° were relatively high compared to spring and summer seasons. These directions correspond to wind direction along the road. Besides, influence of stability on flux footprints can affect the contribution of emissions resulting seasonal differences.

3.2 Temporal variation of particle fluxes

As particle emissions in urban area are driven by traffic and household activity, the particle fluxes are expected to show diurnal variation with differences between weekdays and weekends. Diurnal variation is, in addition, affected by atmospheric mixing conditions, where source-sink relationship between emission areas and flux measurement point is affected by atmospheric stability. Figure 5 shows the diurnal variation of particle fluxes as separated for three distinct surface types. The fluxes were systematically observed to be higher from the road sector reaching 10^9 m^{-2} s^{-1}, and lower from the vegetation sector, where the fluxes stayed below 300×10^6 m^{-2} s^{-1}. Differences in diurnal cycles between seasons were not distinguishable except during weekends, when particle fluxes from road were significantly higher in fall/winter season than in summer and spring.

Particle sources dominated over deposition sink in the vegetation sector (Fig. 5). However, the upward fluxes were systematically lower over this sector indicating weaker emissions in the footprint area. Particle deposition to forested area is expected to be in the order of 10^6 to 10^7 m^{-2} s^{-1} (Pryor et al., 2007), which is an order of magnitude smaller than the observed emissions, and thus deposition has probably minor effect on total particle fluxes. During weekends, particle fluxes from vegetation and urban area were not distinguishable suggesting that on weekdays traffic activity is also the main source of particles on these areas.

The particle flux statistics for different land use types, seasons, weekdays/weekends and day/night are summarised in Table 1. According to observed similarity, data for spring and summer as well as for night-time weekend and weekday was aggregated. In all land use sectors, the highest particle fluxes were measured in fall/winter indicating higher emissions from stationary combustion sources during the colder months. As was evident from the diurnal behaviour, the highest fluxes were measured on weekdays, when the median fluxes ranged between 120 and 840×10^6 m^{-2} s^{-1}. The particle fluxes were low in night-time ranging from 20 to 110×10^6 m^{-2} s^{-1}. Systematically, the

highest fluxes were measured in the road sector and the lowest in the vegetation sector. These observed differences between different land use areas are similar to those reported by Mårtensson et al. (2006) in Stockholm, Sweden.

The observed particle fluxes are similar to those reported in previous studies, which have varied between 200 and $1200\times10^6\,\mathrm{m^{-2}\,s^{-1}}$ (Dorsey et al., 2002; Mårtensson et al., 2006; Nemitz et al., 2008). Direct comparisons are, however, difficult since other studies have measured particles starting from 11 nm, and besides particle fluxes are highly dependent on the measurement location, height and the intensity of traffic, which vary strongly between different studies.

3.3 Traffic rate dependence

Figure 6 shows traffic rate (*Tr*) at Itäväylä road (adjusted to the road next to the measurement station) indicating strong diurnal variation, but little difference between seasons. An hourly shift can be observed in traffic rates due to change to summer time for spring and summer seasons. Evidently, traffic rate variation correlated with the diurnal particle fluxes (see also Fig. 5) as has also been observed by Dorsey et al. (2002) and Mårtensson et al. (2006). We also correlated particle fluxes with traffic rate in the road sector (Fig. 7), and approximated the dependence with exponential curve similarly to Dorsey et al. (2002), despite the fact that distinction between linear or exponential dependence could not be done based on current measurements. Direct emissions from traffic should be proportional to traffic count, thus, suggesting linear dependence, but e.g. correlation of traffic rate with stability could cause dependence other than linear. Especially the particle fluxes corresponding to traffic rates around 2000 counts per hour showed large variability. This traffic rate corresponds to daytime situations (11:00–13:00), when the atmosphere is most unstable. To get more information about the effect of mixing conditions on measured fluxes, particle fluxes normalized with traffic counts as a function of atmospheric stability for the road sector were plotted in Fig. 8. The normalized particle fluxes showed wide range of variability, but systematic average dependence on stability parameter could be observed. Results indicate that

unstable conditions favour stronger dependence between traffic emissions and measured flux. Part of the non-linearity between the particle fluxes and traffic rates could also be explained by other factors not included into the analysis, like heavy duty traffic, which is high at the road next to the measurement site. Heavy duty vehicles were not accounted separately in traffic rate calculations, and since the particle emissions are higher from these vehicles (Ban-Weiss et al., 2009), ignoring them could cause nonlinearity between particle flux and traffic count.

3.4 Footprint and road source analysis

Figure 1 shows the isolines of the calculated flux footprint function, i.e. the function relating the contribution of surface source to measured flux (e.g. Schmid, 2002). The flow pattern was strongly affected by buildings, and therefore the footprint function of surface fluxes showed a complicated pattern, which did not follow the smooth pattern characteristic to horizontally homogeneous conditions. In contrast to horizontally homogeneous conditions, the function had two local maxima, one close to the measurement tower and another one at longer distance. Model simulations also indicated that the footprint function was highly sensitive to wind direction.

Figure 9 presents the flux footprint function in cross-wind integrated form as estimated by numerical (SCADIS model) and analytical (Horst and Weil, 1994) models. Note that application of analytical model to such conditions can only be indicative, and it is used for comparison purposes, how the footprint function would look like under horizontally homogeneous conditions. The footprint maximum of the numerical simulation is shifted due to topography when compared to the analytical simulation.

From measured flux F_p and cross-wind integrated footprint function value $F_y(x)$ at distance x upwind from measurement location, the line source strength L in $\mathrm{m^{-1}\,s^{-1}}$ can be estimated as $L(x)=F_pF_y(x)^{-1}$. The estimated L can be used to approximate the traffic emission rate. By taking the flux from road direction equal to $800\times10^6\,\mathrm{m^{-2}s^{-1}}$ and using a rough footprint value $F_y(150\,\mathrm{m})=10^{-3}\,\mathrm{m^{-1}}$ (Fig. 9), the average source

strength of the road was estimated to be 0.8×10^{12} m^{-1} s^{-1}. Assuming further the average speed of cars to be equal to 40 km h^{-1} and using Tr=2500 hr^{-1}, the previous result yielded for an average emission rate per car as 1.3×10^{13} s^{-1}, which is equivalent to 1.2×10^{15} vehicles^{-1} km^{-1}. This is in a good agreement with Zhu and Hinds (2005) who estimated the particle emission rate to be 5.2×10^{14} vehicle^{-1} km^{-1} or 2×10^{12} m^{-1} s^{-1} at Interstate 405 Freeway with traffic rate about 13 800 vehicles hr^{-1}. They reported the average speed of vehicles to be 97 km h^{-1}, which explains the lower emission rate per vehicle per km. Another study by Gramotnev et al. (2003) determined average emission rate on a busy road in Australia with traffic rate between 3000 and 3500 vehicles per hour to equal 2.8×10^{14} vehicle^{-1} km^{-1}. It should be noted that Gramotnev et al. (2003) determined the emission factor based on the concentration measurements between 15 nm and 0.7 µm whereas our measurements extend down to 6 nm.

The advantage of estimating the emission factor from particle flux measurements using the footprint approach, or from concentration measurements using dispersion modelling as done by Zhu and Hinds (2005) and Gramotnev et al. (2003), is the generality of the result in terms of emission per vehicle per km of road. As discussed and summarised by Martin et al. (2008), the particle flux measurements at different cities can be related directly to traffic rate and friction velocity, however, such relationships would include site specific proportionality coefficient related to location and height of the flux measurement system.

3.5 Correlation between particle and carbon dioxide fluxes

Correlation analysis between particle fluxes and carbon dioxide (CO_2) fluxes indicated similarity of respective sources (Table 2). During the growing season, vegetation acts as carbon sink during day-time, lowering the overall EC flux. This yielded lower correlation for particle and CO_2 flux since particle fluxes are not affected by vegetation uptake as much. Especially in the vegetation sector, the uptake could exceed CO_2 emissions resulting negative fluxes. To exclude CO_2 uptake period from correlation

analysis, only data points with CO_2 fluxes greater than zero were used. In fall/winter, the fluxes showed similar dependence for all land use sectors, i.e. the particle emission was proportional to CO_2 emission. In the road sector, the correlation between the fluxes was the strongest with squared R varying from summery 0.47 to spring time 0.71. For urban and vegetation sectors the correlations were below 0.41 except in the vegetation sectors in winter/fall when the squared R reached 0.63. Nemitz et al. (2008) found also low dependence between particle and CO_2 fluxes in Boulder, Colorado, in summer time.

3.6 Size dependence of the particle fluxes

The EC system measures an integral flux of wide range of particle sizes. Geometric mean diameter (GMD) of the particle size spectrum was calculated from the twin DMPS data to gain information about the relationship between particle sizes and fluxes. In the road direction, the highest particle fluxes correlated with the smallest particle sizes (Fig. 10), while for other directions this was not observed. Such dependence was caused by spring and fall/winter data, while in summer the GMD variation range under selected conditions was limited to larger values and trend could not be observed. The result agrees with Schmidt and Klemm (2008) who found the particle fluxes increasing with decreasing particle size, and supports also the previous founding's that road traffic is a major source for ultrafine particles (Young and Keeler, 2007; Järvi et al., 2009).

4 Conclusions

The temporal behaviour of aerosol particle number fluxes together with the dependencies on land use and traffic rate were studied in Helsinki, Finland in July 2007–July 2008. Besides the effect of mixing conditions, relationship between the fluxes and particle sizes and correlation between particle and CO_2 fluxes were analyzed.

The highest particle fluxes were measured in winter/fall, when the medians ranged

between 110 and 840×10^6 m^{-2} s^{-1} during daytime on weekdays. This is due to enhanced emissions from stationary emission sources during colder months. Fluxes had a distinct dependence on land use with the highest values in the road sector reaching 840×10^6 m^{-2} s^{-1} in daytime on weekdays, and the lowest in the vegetation sector where the fluxes remained below 230×10^6 m^{-2} s^{-1}. The lower fluxes in vegetation sector were due to the low amount of anthropogenic sources on the area, and particle deposition on vegetation was likely to have only minor effect on the measured fluxes.

The diurnal cycle of particle fluxes followed closely traffic patterns similarly as reported in previous studies (Dorsey et al. 2002; Mårtensson et al. 2006). Besides traffic rate, a clear dependence with the atmospheric mixing conditions was observed. Higher particle fluxes correlated with smaller particle sizes in the road sector supporting previous findings that road traffic is a source especially for ultrafine particles (Young and Keeler, 2007; Järvi et al., 2009). Correlation between particle and CO_2 fluxes was good especially in the road sector indicating similarity in sources. Numerical atmospheric boundary-layer model with sophisticated topography and land use description was used for air flow and flux footprint modeling. By using the calculated footprint function, the emission rate from the road was estimated to be 0.8×10^{12} m^{-1} s^{-1} or 1.2×10^{15} vehicles^{-1} km^{-1}.

Acknowledgement. We would like to thank Maj and Nessling foundation, National technology Agency (TEKES, Ubicasting project) and Helsinki University Environmental Research Centre (HERC) for financial support. This work was also supported by the Academy of Finland Center of Excellence program (project number 1118615) and European Commission (Projects CARBOEUROPE, IMECC, ICOS and BRIDGE).

References

Aalto, P., Hämeri, K., Becker, E., Weber, R., Salm, J., Mäkelä, J., Hoell, C., O'Dowd, C., Karlsson, H., Hansson, H.-C., Väkevä, M., Koponen, I. K., Buzorius, G., and Kulmala, M.: Physical characterization of aerosol particles during nucleation events, Tellus B, 53, 344–358, 2001.

Ban-Weiss, G. A., Lunden, M. M., Kirchstetter, T. W., and Harley, R. A.: Measurement of black carbon and particle number emission factors from individual heavy duty vehicles, Environ. Sci. Technol., 43, 1419–1424, 2009.

Baron, P. A. and Willeke, K.: Aerosol Measurement: Principles, techniques, and applications, 2nd edition, John Wiley & Sons, New York, 2001.

Curtis, L., Rea, W., Smith-Willis, P., Fenyves, E., and Pan, Y.: Adverse health effects of outdoor air pollutants, Environ. Int., 32, 815–830, 2006.

Donateo, A., Contini, D., and Belosi, F.: Real time measurements of PM2.5 concentrations and vertical turbulent fluxes using an optical detector, Atmos. Environ., 40, 1346–1360, 2006.

Dorsey, J., Nemitz, E., Gallagher, M., Fowler, D., Williams, P., Bower, K., and Beswick, K.: Direct measurements and parametrisation of aerosol flux, concentration and emission velocity above a city, Atmos. Environ., 36, 791–800, 2002.

Glasius, M., Ketzel, M., Wåhlin, P., Jensen, B., Mønster, J., Berkowicz, R., and Palmgren, F.: Impact of wood combustion on particle levels in a residential area in Denmark, Atmos. Environ., 40, 7115–7124, 2006.

Gramotnev, G., Gramotneva, G., Brown, R., Ristovski, Z., Hitchins, J., and Morawska, L.: Determination of average emission factors for vehicles on a busy road, Atmos. Environ., 37, 465–474, 2003.

Horst, T. W. and Weil, J. C.: How far is far enough? The fetch requirements for micrometeorological measurement of surface fluxes, J. Atmos. Oceanic Technol., 11, 1018–1025, 1994.

Horst, T. W.: A simple formula for attenuation of eddy fluxes measured with first-order-response scalar sensors, Bound.-Lay. Meteorol., 82, 219–233, 1997.

Intergovernmental Panel on Climate Change: Climate Change 2007: The Physical Science Basis, Contribution of Working group I to the Fourth Assessment Report of the Intergovernmental Panel on Climate Change, edited by: Solomon et al., Cambride University Press, 2007.

Järvi, L., Hannuniemi, H., Hussein, T., Junninen, H., Aalto, P. P., Hillamo, R., Mäkelä, T., Keronen, P. Siivola, E., Vesala, T., and Kulmala, M.: The urban measurement station SMEAR III: Continuous monitoring of air pollution and surface-atmosphere interactions in Helsinki, Finland, Boreal Environ. Res., 14 (Suppl. A), 86–109, 2009.

Kaimal, J. C., Wyngaard, J. C., Izumi, Y., and Coté, O. R.: Spectral characteristics of surface-layer turbulence, Q. J. Roy. Meteor. Soc., 98, 563–589, 1972.

Keeler, G., Morishita, M., and Young, L.-H.: Characterization of complex mixtures in urban

atmospheres for inhalation exposure studies, Exp. Toxicol. Pathol., 57, 19–29, 2005.
Kumar, P., Fennell, P., and Britter, R.: Measurements of particles in the 5–1000 nm range close to road level in an urban street canyon, Sci. Total Environ., 390, 437–447, 2008.
Lilleberg, I. and Hellman, T. Liikenten kehitys Helsingissä vuonna 2007 (in Finnish), Publications by Helsinki City Planning Department, 2008:2, 2008.
Longley, I. D., Gallagher, M. W., Dorsey, J. R., and Flynn, M.: A case-study of fine particle concentrations and fluxes measured in a busy street canyon in Manchester, UK, Atmos. Environ., 38, 3595–3603, 2004a.
Longley, I. D., Gallagher, M. W., Dorsey, J. R., Flynn, M., Bower, K. N., and Allan, J. D.: Street canyon aerosol pollutant transport measurements, Sci. Total Environ., 334–335, 327–336, 2004b.
Martin, C. L., Longley, I. D., Dorsey, J. R., Thomas, M. R., Gallagher, M. W., and Nemitz, E.: Ultrafine particle fluxes above four major European cities, Atmos. Environ., doi:10.1016/j.atmosenv.2008.10.009, 2008.
McMillen, R. T.: An eddy correlation technique with extended applicability to non-simple terrain, Bound.-Lay. Meteorol., 43, 231–245, 1988.
Moore, C. J.: Frequency response corrections for eddy correlation systems, Bound.-Lay. Meteorol., 37, 17–36, 1986.
Mårtensson, E. M., Nilsson, E. D., Buzorius, G., and Johansson, C.: Eddy covariance measurements and parameterisation of traffic related particle emissions in an urban environment, Atmos. Chem. Phys., 6, 769–785, 2006, http://www.atmos-chem-phys.net/6/769/2006/.
Nemitz, E., Fowler, D., Dorsey, J. R., Theobald, M. R., McDonald, A. D., Bower, K. N., Beswick, K. M., Williams, P. I., and Gallagher, M. W.: Direct measurement of size-segregated particle fluxes above a city, J. Aerosol Sci., 31 (Suppl. 1), 116–117, 2000.
Nemitz, E., Jimenez, J. L., Huffman, J. A., Ulbrich, I. M., Canagaratna, M. R., Worsnop, D. R., and Guenther, A. B.: An eddy-covariance system for the measurement of surface/atmosphere exchange fluxes of submicron aerosol chemical species – first application above an urban area, Aerosol Sci. Technol., 42, 636–657, 2008.
Niemi, J., Väkevä, O., Kousa, A., Weckström, M., Julkunen, A., Myllynen, M., and Koskentalo, T.: Air Quality in the Helsinki Metropolitan Area in 2007 (in Finnish), YTV Helsinki Metropolitan Area Council, 8/2008, 2008.
Pakkanen, T., Loukkola, K., Korhonen, C. H., Aurela, M., Mäkelä, T., Hillamo, R., Aarnio, P.,

Koskentalo, T., Kousa, A., and Maenhaut, W.: Sources and chemical composition of atmospheric fine and coarse particles in the Helsinki area, Atmos. Environ., 35, 5381–5391, 2001.
Palmgren, F., Berkowicz, R., Ziv, A., and Hertel, O.: Actual car fleet emissions estimated from urban air quality measurements and street pollution models, Sci. Total Environ., 235, 101–109, 1999.
Pryor, S. C., Larsen, S. E., Sørensen, L. L., Barthelmie, R. J., Grönholm, T., Kulmala, M., Launiainen, S., Rannik, Ü., and Vesala, T.: Particle fluxes over forests: Analyses of flux methods and functional dependencies, J. Geophys. Res., 112, D07205, doi:10.1029/2006JD008066, 2007.
Pryor, S. C., Gallagher, M., Sievering, H., Larsen, E., Barthelmie, R. J., Birsan, F., Nemitz, E., Rinne, J., Kulmala, M., Grönholm, T., Taipale, R., and Vesala, T.: A review of measurement and modelling results of particle atmosphere–surface exchange, Tellus B, 60, 42–75, 2008.
Rannik, Ü. and Vesala, T.: Autoregressive filtering versus linear detrending in estimation of fluxes by the eddy covariance method. Bound.-Lay. Meteorol., 91, 259–280, 1999.
Rannik, Ü., Keronen, P. Hari, P., and Vesala, T.: Estimation of forest-atmosphere CO_2 exchange by eddy covariance and profile techniques, Agr. Forest Meteorol., 126, 141–155, 2004.
Schmid, H. P.: Footprint modeling for vegetation atmosphere exchange studies: a review and perspective, Agr. Forest Meteorol., 113, 159–183, 2002.
Schmidt, A. and Klemm, O.: Direct determination of highly size-resolved turbulent particle fluxes with the disjunct eddy covariance method and a 12 – stage electrical low pressure impactor, Atmos. Chem. Phys., 8, 7405–7417, 2008, http://www.atmos-chem-phys.net/8/7405/2008/.
Sogachev, A., Menzhulin, G., Heimann, M., and Lloyd, J.: A simple three-dimensional canopy–planetary boundary layer simulation model for scalar concentrations and fluxes, Tellus B, 54(5), 784–819, 2002.
Sogachev, A. Y. and Lloyd, J. J.: Using a one-and-a-half order closure model of the atmospheric boundary layer for surface flux footprint estimation, Bound.-Lay. Meteorol., 112, 467–502, 2004.
Sogachev, A., Rannik, Ü., and Vesala, T.: On flux footprints over the complex terrain covered by a heterogeneous forest, Agric. For. Meteorol., 127, 143–158, 2004.
Sogachev, A. and Panferov, O.: Modification of two-equation models to account for plant drag, Bound.-Lay. Meteorol., 121, 229–266, 2006.

Sogachev, A.: A note on two-equation closure modelling of canopy flow, Bound.-Lay. Meteorol., 130, 423–435, DOI: 10.1007/s10546-008-9346-2, 2009.

Thomas, S. and Morawska, L.: Size-selected particles in an urban atmosphere of Brisbane, Australia, Atmos. Environ., 36, 4277–4288, 2002.

Vesala, T., Järvi, L., Launiainen, S., Sogachev, A., Rannik, Ü., Mammarella, I., Siivola, E., Keronen, P., Rinne, J., Riikonen, A., and Nikinmaa, E.: Surface-atmosphere interactions over complex urban terrain in Helsinki, Finland, Tellus B, 60, 188–199, 2008.

Zhu, Y. and Hinds, W. C.: Predicting particle number concentrations near a highway based on vertical concentration profile, Atmos. Environ., 39, 1557–1566, 2005.

Young, L.-H. and Keeler, G.: Summertime ultrafine particles in urban and industrial air: aitken and nucleation mode particle event, Aerosol Air Qual. Res., 7, 379–402, 2007.

Table 1. Median aerosol particle fluxes (in $10^6\,m^{-2}\,s^{-1}$) for different seasons, land use sectors and separately for day- and night-time. The respective quartile deviations are also listed.

	Spring/Summer			Winter/Fall		
	Urb	Road	Veg	Urb	Road	Veg
Weekday daytime (10:00–15:00)	180±149	663±271	119±79	321±277	837±348	232±132
Weekend daytime (10:00–15:00)	55±43	309±127	44±26	91±57	511±224	85±46
Weekday+Weekend night-time (23:00–04:00)	19±14	39±26	16±9	40±20	109±62	35±19

Table 2. Correlation statistics from the linear regression made between aerosol particle flux F_p (in 10^6 m^{-2} s^{-1}) and carbon dioxide flux F_c (in µmol m^{-2} s^{-1}) for F_c>0 (to exclude carbon dioxide uptake in vegetation direction in spring and summer seasons). Regressions were determined for 30-min average flux values.

	Urb	Road	Veg
Summer	F_p=10F_c+32, R^2=0.16	F_p=28F_c+63, R^2=0.47	F_p=18F_c−14, R^2=0.14
Fall/Winter	F_p=50F_c−34, R^2=0.35	F_p=46F_c+60, R^2=0.66	F_p=46F_c−40, R^2=0.63
Spring	F_p=51F_c−58, R^2=0.32	F_p=37F_c+8, R^2=0.71	F_p=29F_c+3, R^2=0.41

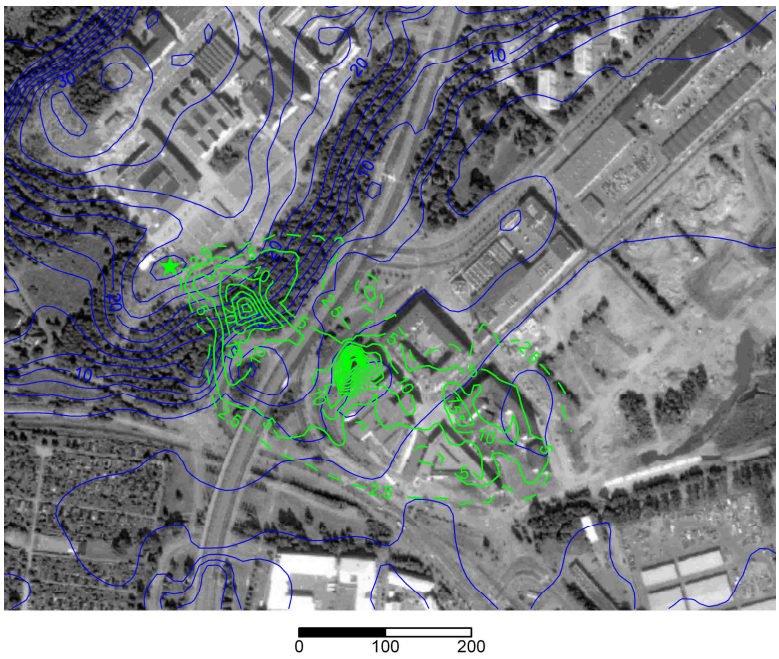

Fig. 1. Aerial photograph of the measurement surroundings. Topography of the measurement site is drawn by blue contours indicating the height relative to sea level. Green contours give flux footprint function (scale 10^{-6}, the unit of flux footprint is m^{-2}) for surface sources for flux measurements from road direction. The location of the measurement tower is marked with green star and the distance to the road is around 150 m.

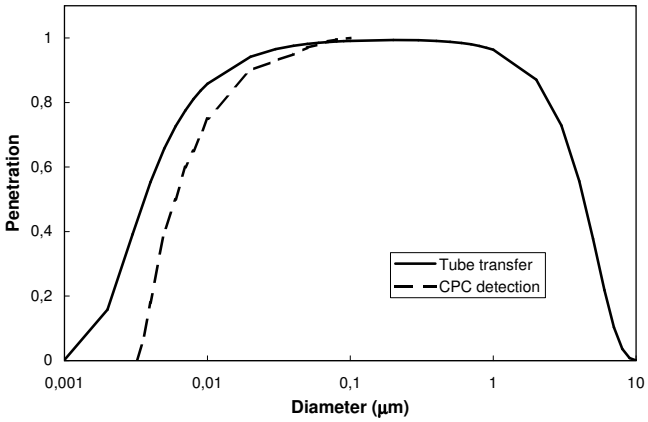

Fig. 2. Particle size transfer function of the particle EC system. In penetration calculation according to Baron and Willeke (2001), tube was assumed to consist of 10 different segments including bendings. Density of particles was assumed to be 1.5 g cm^{-3}.

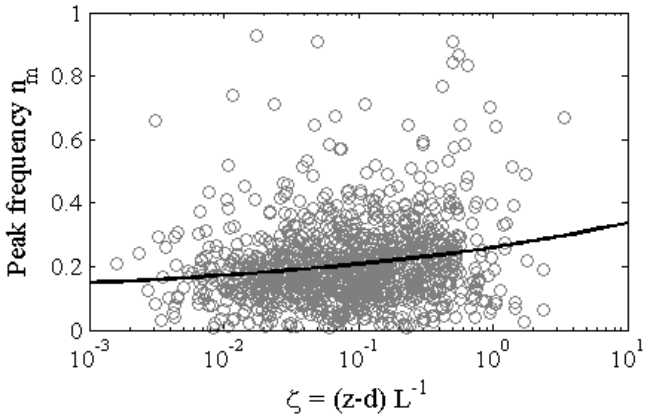

Fig. 3. The normalized peak frequency n_m as a function of atmospheric stability ζ for stable stratification cases calculated for April–August 2007. Circles show the half hour data points and black solid line is the fitted line corresponding to Eq. (3).

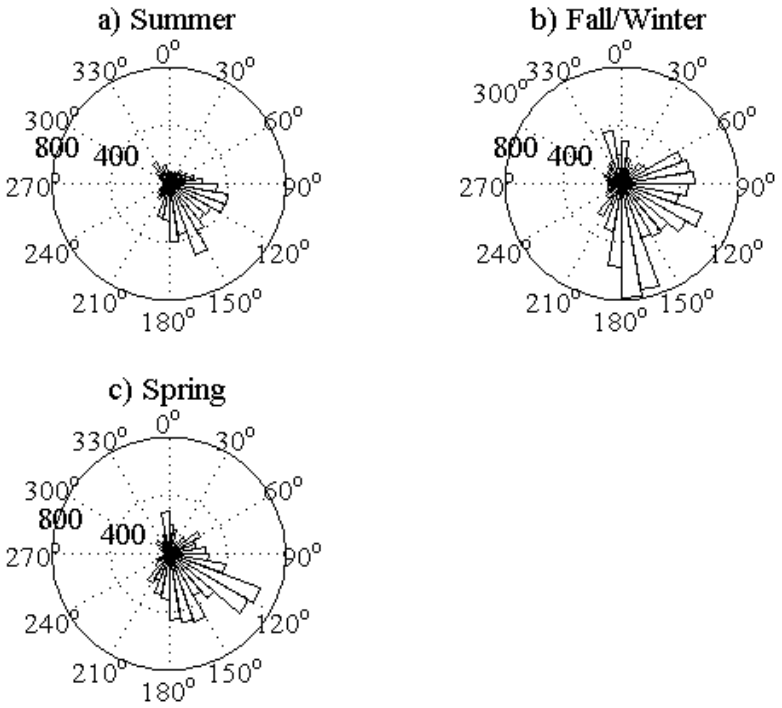

Fig. 4. The wind direction dependence of aerosol particle number fluxes (F_p) for **(a)** summer, **(b)** fall/winter and **(c)** spring. Values were calculated for 10° wind sectors as medians from 30-min average fluxes. The units are in 10^6 m^{-2} s^{-1}.

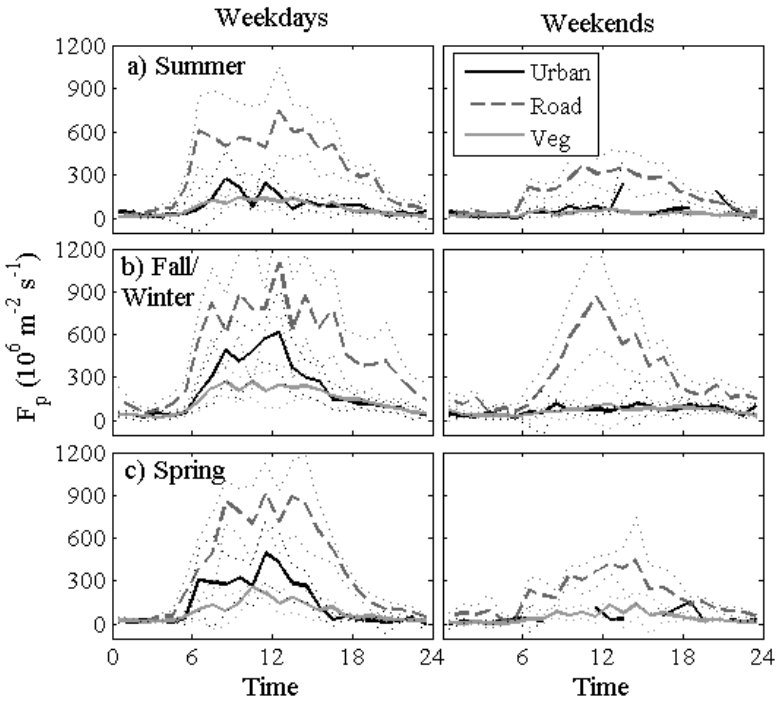

Fig. 5. The median diurnal behaviour of aerosol particle number fluxes (F_p) for different seasons and land use sectors and for weekdays and weekends separately. Dotted lines present the quartile deviations.

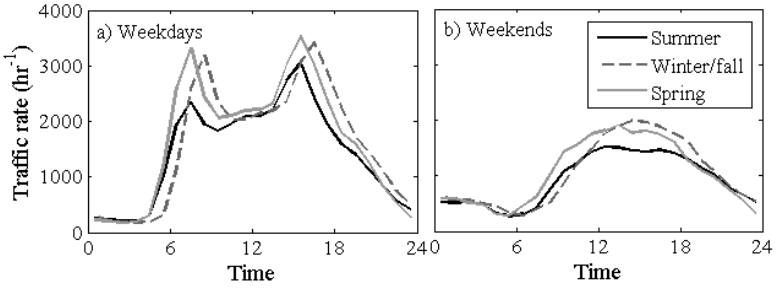

Fig. 6. Diurnal variation of traffic rate on **(a)** weekdays and **(b)** weekends measured by the Helsinki City Planning Department at Itäväylä road (adjusted to the road next to the measurement station) between July 2007 and May 2008.

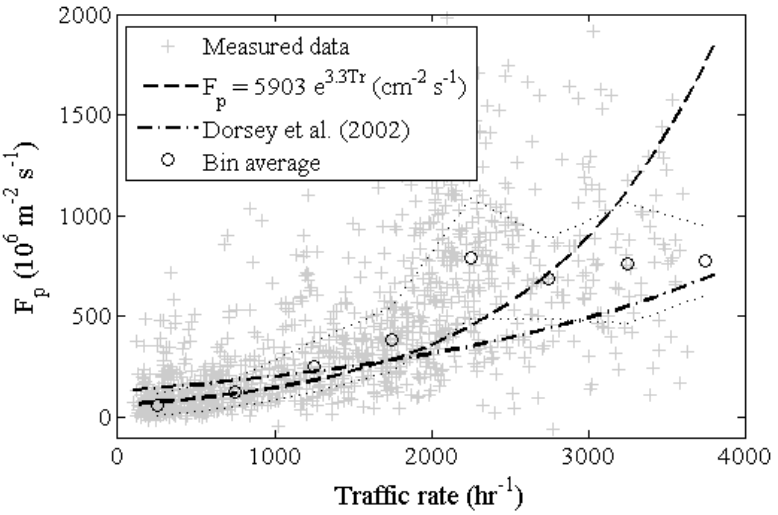

Fig. 7. Hourly correlation between particle number flux (F_p) and traffic rate in July 2007–May 2008. Grey crosses show the hourly particle fluxes, dashed line shows the exponential fitting (F_p=5903$e^{3.3Tr}$ in cm^{-2} s^{-1}) made to the data points and dash-dot line is the fitting (F_p=13000$e^{1.8Tr}$ in cm^{-2} s^{-1}) obtained by Dorsey et al. (2002) in City of Edinburgh. Circles are the median values calculated for 500 vehicles h^{-1} bins, dotted lines represent the quartile deviations.

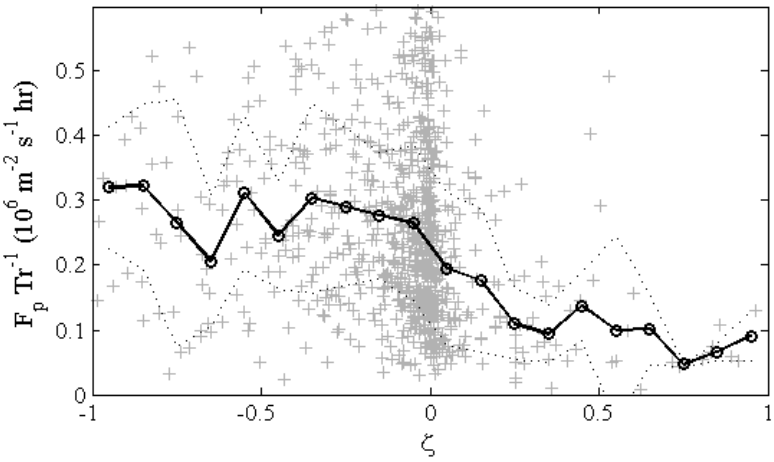

Fig. 8. Particle fluxes normalised with traffic rate (F_p Tr^{-1}) as a function of atmospheric stability ζ. Data was plotted for wind direction 40–180° during July 2007 and May 2008. Circles are the median values and dotted lines represent the quartile deviations.

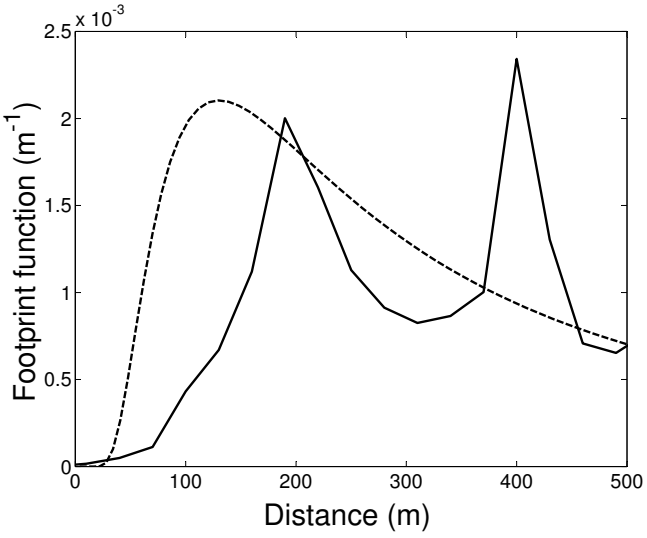

Fig. 9. Cross-wind integrated flux footprint as estimated for surface sources in road direction from analytical (dashed line, according to Horst and Weil, 1994) and numerical models (solid line). Neutral stratification and measurement height of 31 m were assumed.

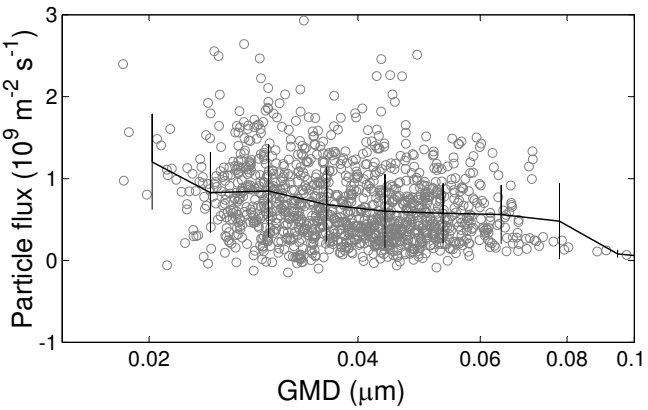

Fig. 10. Particle fluxes vs. geometric mean diameter (GMD) during work hours in the road sector on weekdays.